NASA MEMO 5-3-59L

NASA

MEMORANDUM

INVESTIGATION OF THE STRUCTURAL BEHAVIOR AND MAXIMUM BENDING STRENGTH OF SIX MULTIWEB BEAMS WITH THREE TYPES OF WEBS

By James P. Peterson and Walter E. Bruce, Jr.

Langley Research Center
Langley Field, Va.

NATIONAL AERONAUTICS AND SPACE ADMINISTRATION

WASHINGTON

May 1959

NATIONAL AERONAUTICS AND SPACE ADMINISTRATION

MEMORANDUM 5-3-59L

INVESTIGATION OF THE STRUCTURAL BEHAVIOR AND MAXIMUM BENDING STRENGTH OF SIX MULTIWEB BEAMS WITH THREE TYPES OF WEBS

By James P. Peterson and Walter E. Bruce, Jr.

SUMMARY

The results of bending tests on six multiweb beams of optimum weight-strength design are presented. The internal structure of the beams consisted of various combinations of two types of full-depth solid webs and a post-stringer web. The observed structural behavior, buckling load, and failing load of the beams are compared with results obtained by the use of existing methods of analysis and found to be quite predictable.

INTRODUCTION

Various schemes for supporting the covers of aircraft wings are in general use and considerable effort is often required in order to determine the supporting structure that should be employed in a given design. Weight-strength diagrams provide a rational basis for selecting a supporting structure but the computations necessary to construct such a diagram usually make use of expedient assumptions that may affect the validity of the computations in regions of optimum design where every component of the structure is being worked to its limit. Confidence in the diagrams can be bolstered appreciably, therefore, if they are verified by the results of a few tests on structures closely simulating those predicted by the diagrams, and such tests often supplement analytical weight-strength analyses.

Wings of skin-stringer-rib construction are lighter than those of multiweb construction if the design requires deep wings. If the design requires shallow wings multiweb construction is the lighter, and at some range of intermediate depths designs of nearly equal weight result. Furthermore, in this intermediate range, a design of equally light weight can be obtained with a type of construction employing a combination of skin-stringer construction and multiweb construction (see ref. 1). Wings of

this construction are called multipost-stiffened wings and have the advantage of providing greater accessibility to the interior of the wings during fabrication than either skin-stringer or multiweb construction by itself.

The general problem of multipost-stiffened wings is treated theoretically in references 2 to 5 and design charts are presented in reference 5 which facilitate considerably the design of a class of multipost-stiffened wings in which alternate full-depth webs of a multiweb wing are replaced by stringers and posts. References 1 and 6 report some tests on three-web beams with the middle web replaced by posts and stringers. The conclusion drawn from the results of each set of tests is that the experimental results are fundamentally in agreement with the theory presented in references 4 and 5.

The present paper reports the results of tests on 6 seven-web beams subjected to bending. The supporting structures of the beams feature two types of full-depth solid webs and combinations of these webs and post-stringer webs. The beams are of nearly optimum design for a given ratio of beam depth to face-sheet thickness and thereby provide a severe check on the reliability of weight-strength computations for such structures.

SYMBOLS

A	cross-sectional area of test beam effective in resisting axial or bending loads, sq in.
A_C	cross-sectional area of that part of test beam considered to be compression cover and supporting structure, including equivalent area of posts, sq in.
A_i	cross-sectional area per chordwise inch of multiweb beam considered to be compression cover and supporting structure, in.
b_S	web spacing, in.
c	distance from neutral axis to extreme compression fiber of beam, in.
E	Young's modulus, ksi
h	beam depth measured from outside of compression cover to outside of tension cover, in.
I	moment of inertia of test beam, $in.^4$

M_e	equivalent applied moment, in-kips
M_f	equivalent applied bending moment at beam failure, in-kips
$M_{f,calc}$	calculated bending moment at beam failure, in-kips
M_i	bending moment at failure per chordwise inch of multiweb beam, kips
P	applied jack load, kips
t_S	thickness of compression cover, in.
t_T	thickness of tension cover, in.
t_W	web thickness, in.
w	width of tension and compression covers of test beams, in.
α	web stress-distribution coefficient
$\bar{\epsilon}$	unit shortening
ϵ_2	strain at which tangent modulus equals one-half secant modulus
ϵ_{cr}	computed strain in compression cover when cover buckling occurred, ksi
σ_{cr}	stress in compression cover when cover buckling occurred, ksi

TEST SPECIMENS

The test specimens consisted of six multiweb beams fabricated from 7075-T6 aluminum alloy. The beams were 10 inches deep with internal supporting structures (webs) that varied from beam to beam. The three types of webs used are shown in figure 1. They include two types of conventional full-depth webs and a post-stringer web composed of inverted hat-shaped stringers and small channel-shaped posts spaced at 6-inch intervals along the beam. The posts were connected to the stringers by means of a single snug-fitting aircraft bolt. (See figs. 1 and 2.) The post-stringer webs were only slightly heavier than the conventional webs with an angle connector and were somewhat lighter than the conventional webs with a tee-cap connector.

The arrangement of the webs in each beam is shown schematically in figure 3. These arrangements were chosen in order to study (1) the effect of replacing one-half or two-thirds of the conventional webs of a multiweb beam with post-stringer webs and (2) the utility of an angle connection as opposed to a tee-cap connection between conventional full-depth webs and the covers of multiweb beams. Pertinent dimensions of the beams are given in table I.

Beams 1 and 4 were designed to have nearly optimum proportions for a ratio of beam depth to compression-cover thickness h/t_S of 40. This value was chosen as representative of the range in which post-stringer webs compete with solid conventional webs. The relative efficiency of three sections, two of which are representative of those of beams 1 and 4, is given in figure 4 by plots of $\sqrt{M_1}/A_1$ against M_1/h^2. The curves are for beams of optimum proportions from a weight-strength point of view and were obtained by using the procedures established in reference 7 with one exception. A value of 1/6 was used for the web stress-distribution coefficient α instead of the value of 1/4 used in reference 7. The value 1/6 corresponds to a linear (Mc/I) stress distribution. For all practical purposes the value 1/6 is consistent with the observation, which forms the basis of the procedure of reference 7, that the cover fails when the edge strain reaches ϵ_2. That is, the amount of nonlinearity in the stress-strain curve for the structural aluminum alloys is small for strains less than ϵ_2 (see ref. 8), and the use of a linear stress distribution should represent quite accurately the stress field in the webs at failure. This expectation is substantiated by the results of the present investigation as well as by those of reference 7.

The three sections considered in figure 4 are nearly equally efficient, as indicated by the closeness of the various curves. Beam proportions are different for each value of M_1/h^2 in figure 4. The main variable is b_S/t_S, which decreases as M_1/h^2 increases. The web thickness also varies, being only great enough, at any value of M_1/h^2, to prevent web crushing and web buckling. Values of M_1/h^2 associated with a value of b_S/t_S of 29 (the value used ir the test beams) are indicated by the vertical lines in figure 4.

Beams with a value of b_S/t_S of 29 were chosen for testing in preference to beams with a larger value of b_S/t_S which would have been just as efficient strengthwise (note that beams with b_S/t_S of 29 are somewhat to the right of the maximum of the curves of fig. 4). Beams with a larger value of b_S/t_S would have experienced more buckling at

loads near maximum load. More buckling might be less desirable for some applications, particularly if it were to occur below limit load or if it were to reduce the torsional stiffness of the structure to an intolerable level. A value of t_w/t_s of 0.45 was computed as the minimum value that should be used for beams of the proportions tested. The use of a smaller value could lead to designs having excessive web buckling, which might induce a premature failure. A nominal value of 0.41 was actually used in order that sheets of standard gage could be utilized.

The post-stringer webs of beams 2, 3, 5, and 6 were designed, according to the design charts of reference 5, to be functionally equivalent to the solid webs which they replaced. They were designed to have adequate stiffness to provide the equivalent of simple support to the cover along the line of attachment between the cover and the post-stringer web. In addition, the posts were designed to have adequate column strength to carry the crushing loads induced by beam curvature. The area of post required for each of these functions was so small that posts with an area about an order of magnitude larger than the calculated area were actually used in order that members of practical size could be used.

TEST PROCEDURE

Photographs of typical test setups are shown in figures 5 and 6. The principal components of the setups are: (1) the test beam, (2) the loading frame, (3) the loading jack, (4) the counter balancing system, and (5) the data recorder.

The setups of figures 5 and 6 differ mainly in that the direction of applied load in one case is vertical (fig. 5) and in the other case is skewed 22° from the vertical (fig. 6). Beams 1 and 2 were tested in the rig as illustrated in figure 5. The bending deformation of these beams at loads near failure caused a rotation of the loading frame as depicted (somewhat exaggerated) in the sketch of figure 7, which necessitated moving the loading jack in the course of the test of beam 2 in order to keep the ram of the jack in contact with the loading pedestal.

Moving the jack was avoided in the remaining tests by poising the jack at an angle which kept the relative motion between the jack and loading pedestal small. However, in this case the rig applies a tension load to the test beam as well as a bending load, and beams 3 to 6 were fabricated with a heavier tension cover to accommodate the additional load. The rig also applies a small vertical shear load to the test beam, which is proportional to the deflection of the tip (end nearer loading frame) of the beam. The shear load is resisted by a correspondingly small moment in the beam which subtracts from the applied moment and which

varies linearly along the beam from zero at the tip of the beam. As a consequence, buckling and failure usually emanated from the region near the tip of the beams.

The presence of stray loads in the test beams was minimized as far as practicable by employing rollers between moving surfaces and by counterbalancing fixtures near their center of gravity. Rollers were used between the loading frame and the floor supports as well as between the loading frame and the testing machine to allow the beams to shorten during loading and to restrict the loads at these locations to normal loads. The rollers were case hardened, as were the surfaces against which they reacted. Stray loads not eliminated by counterbalancing and by the use of rollers were considered in reducing the data, including a 4-percent correction for friction which has been determined to be a representative value for the loading frame.

Resistance-type wire strain gages were mounted at various locations on the beams prior to testing, and strains from the gages were autographically recorded during each test with a 24-channel strain recorder. Two types of gages were used. Gages with a 13/16-inch gage length were used on the compression cover of the beams to detect local buckling, and were also used on the stringers of the post-stringer webs and on the attachment angles of the solid webs to indicate the stress in these members. Gages with a 6-inch gage length were used on the tension cover and on the compression cover near lines of internal support to indicate the deformation and stress distribution of the beams.

The tip deflection of some of the beams was autographically recorded as a function of load by the use of resistance-type wire strain gages mounted on small cantilever beams whose deflection was equal to that of the test beam. These measurements were used in determining the vertical shear acting on the beams, as discussed earlier.

TEST RESULTS

Information that is useful in assessing the behavior of a structure includes the response of the structure to load (which is best indicated by a load-deformation curve), the buckling stress and buckling mode, and, the failing stress and failing mode. Data on each of these structural phenomena were obtained.

Load-Shortening Curves

Plots of jack load against unit shortening of the compression and tension covers of each of the test beams are given in figure 8. Unit

shortening for the compression covers was taken from the data obtained with 6-inch strain gages located near the support lines of full-depth webs where nodal lines in the buckling pattern were expected. Unit shortening for the tension covers was taken from data obtained with strain gages located some distance from lines of web support, away from the influence of rivet holes.

The difference in slope between the tension and compression curves for beams 3 to 6 results from dissymmetry of the beams (tension cover heavier than compression cover). The difference in slope is not large. It is less than it would have been if the beams had been tested in pure bending, without end thrust. Consequently, beam behavior, insofar as the compression cover and its supporting structure are concerned, is nearly equivalent to that of a beam with a tension cover equal to the compression cover and loaded in pure bending.

Plots like those of figure 8 are not well adapted for use in assessing beam behavior or in comparing the behavior of one beam with another. Figure 9 has been prepared for this purpose. For beams 1 and 2, the moment M_e in figure 9 is simply the applied moment. For beams 3 to 6, it represents the applied moment reduced by an amount that compensates for the tensile load acting on the beams. The section modulus I/c used in preparing figure 9 is the value computed for the unbuckled elastic structure. Use of this value after initial buckling gives stresses $\bar{\sigma}$ that are nearly a weighted average of the stresses in the compression cover and attachment members. This value is used here rather than a value which gives the average stress in the compression cover or a value which gives the stress in the cover along lines of attachment (so-called edge stress) in order to present load-shortening curves which are as free as possible of computation, yet retain a high degree of usefulness. Other values of the section modulus depend upon the effectiveness of the buckled plate in resisting compression; that is, they depend upon effective-width calculations.

The slopes of all the curves in figure 9 are nearly equal to one another and to Young's modulus E which attests to the validity of the curves as well as to the rational behavior of the beams. The curve for beam 1 is shown dashed above a stress $\bar{\sigma}$ of about 44 ksi. At this point in the testing of this beam the load axis of the recording equipment malfunctioned, and thus the only data available for constructing the dashed portion of the curve was the load at failure, which was read directly from the testing machine, and the strain at failure (the strain axis of the recording equipment continued to function).

The curves of figure 9 terminate at beam failure. The edge strain (strain in compression cover near lines of web support) at failure was in each instance approximately ϵ_2, which for 7075-T6 aluminum-alloy

sheet is taken to be 0.00645. (See ref. 8.) The largest deviation from ϵ_2 at beam failure was observed in beam 1, which failed when the edge strain was approximately 10 percent less than ϵ_2.

Buckling

Each of the beams experienced local buckling of the compression cover at a moment 10 to 15 percent less than that required for failure of the beam. The buckle pattern was in each case characterized by nodal lines along each web, with successive in-and-out buckles along and across the beam (local buckles).

Experimental buckling stresses obtained by the strain-reversal method (see ref. 9) are indicated in figure 9 by short horizontal dashed lines. No buckling stress is indicated for beam 1 because the recording equipment malfunctioned in testing this beam before strain reversal occurred. The test log for this beam indicates that buckling was observed shortly before failure.

The proportions of the solid-web test beams are such, neglecting whatever effect the attachment members may have on buckling, that the webs should initiate buckling. (See ref. 10.) Accordingly, the webs were observed to buckle earlier than the covers of the test beams. However, web buckling is not indicated in figure 9 because the instrumentation of the webs was inadequate to record their buckling.

Experience in testing solid-web beams has demonstrated that the buckling stress of the compression cover as determined by strain reversal is relatively unaffected by small amounts of web buckling. (See ref. 11.) This fact is exemplified by the present tests and is illustrated in figure 9, where the buckling stresses of the beams may be compared with buckling strains (short vertical dashed lines) computed on the assumption that the webs provided simple support to the covers along lines of attachment. It should be emphasized that the post-stringer webs were designed according to reference 5 to provide simple support to the cover. Figure 9 indicates that the test beams buckled at stresses either very close to, or somewhat greater than, the stress corresponding to computed buckling strain.

Failure

A comparison between calculated and experimental moments at failing is given in table II. Good agreement is indicated. The calculations were made by the procedure of reference 7, which applies to beams that fail by local crippling - that is, beams on which the attachment between the covers and webs is of sufficient stiffness and strength to prevent

other modes of failure at lower loads, such as wrinkling and interrivet buckling as well as actual rivet failures. A web stress-distribution coefficient α of 1/6 was used in the computations.

Photographs of the test beams after failure are given in figures 10 to 15. It is evident that failure was in every case accompanied by rivet fractures and in some cases by considerable tearing or shearing of the compression cover. These accompanying phenomena are believed to be secondary failures associated with the large deformations of the structure as it experienced a local crippling failure (failure resulting from the growth of local buckles). Rivet strength is not believed to have had a marked influence on the strength of the beams in view of the fact that the deformations at failure (see fig. 9) as well as the load at failure (see table II) were consistent with predictions for the local crippling type of failure. This conclusion is further supported by the fact that the failures of all the beams were predicted with about the same accuracy, even though some of the beams had weaker riveting and more broken rivets at beam failure than the rest.

DISCUSSION OF RESULTS

Behavior of the test beams was essentially in agreement with predictions. Response of the beams to load was linear and predictable until local buckling occurred in the compression covers of the beams. Local buckling occurred when the compressive stress in the cover reached the buckling stress for a simply supported plate. After local buckling, response of the beams to load was nonlinear and failure occurred as expected when the edge strain reached approximately ϵ_2. One of the beams failed at an edge strain approximately 10 percent less than ϵ_2. The resulting error in failing stress or failing moment was quite small because the slope of the load-shortening curve just prior to failure is small.

A comparison of the results for beams 1 to 3 with those for beams 4 to 6 is interesting. Beams 1 to 3 had angle connectors and beams 4 to 6 had tee-cap connectors between the covers and webs of the beams. Some manufacturers use the tee-cap connector to bolster the buckling and failing stress of built-up multiweb beams such as those tested, even though the angle connector is preferred from a fabrication point of view. However, in the present tests the tee-caps were little, if any, better than the angles in deterring local buckling or in increasing the failure stress. This result should not be interpreted too generally. A stabilizing effect might be obtained by substituting tee-caps for angles in beams which have heavy webs and connectors and light cover skins or in beams for which a wrinkling type of failure is expected. (See ref. 12.)

Nevertheless, the lack of a stabilizing effect in the present tests indicates that the crippling strength of strongly riveted beams of optimum design can be achieved with the use of angle connectors.

Values of $\sqrt{M_f}/A_c$ are given in table II for each of the test beams. Beams with half of the webs of post-stringer construction are in each instance more efficient than the corresponding beams with all conventional webs. Furthermore, the beams with two-thirds of the webs of post-stringer construction are just as efficient as those with half of the webs of post-stringer construction. This result suggests that the design charts of reference 5 can be used to design beams with two-thirds of the webs of post-stringer construction if proportions are used such as those considered herein, which, according to the charts, provide the equivalent of simple support to the covers. The use of more post-stringer webs is usually avoided because full-depth webs are required to supply shear stiffness and shear strength. The values of $\sqrt{M_f}/A_c$ in table II differ considerably from the values of $\sqrt{M_1}/A_1$ in figure 4. If those in table II are multiplied by $\sqrt{w}$ to make the two more comparable, nearly equal values will be obtained.

SUMMARY OF RESULTS

Results of bending tests on six multiweb beams with various types of internal construction (webs) have been presented. The beams were of nearly optimum design from a weight-strength point of view for a ratio of beam depth to compression-cover thickness of 40. The following results were obtained:

1. Existing methods of analysis were adequate for predicting structural behavior, local buckling, and failure of the beams.

2. Test beams with one-half or two-thirds of the webs of post-stringer construction and the rest of the webs of conventional construction were at least as efficient as test beams with all conventional webs.

3. Built-up multiweb test beams with an angle connector between the web and the compression cover were just as efficient as test beams with a tee-cap connector in resisting local buckling or failure.

Langley Research Center,
National Aeronautics and Space Administration,
Langley Field, Va., February 9, 1959.

REFERENCES

1. Johnson, Aldie E., Jr.: Bending Tests on Box Beams Having Solid- and Open-Construction Webs. NACA TN 3231, 1954.

2. Seide, Paul, and Barrett, Paul F.: The Stability of the Compression Cover of Box Beams Stiffened by Posts. NACA Rep. 1047, 1951. (Supersedes NACA TN 2153.)

3. Seide, Paul: Derivation of Stability Criterions for Box Beams With Longitudinally Stiffened Covers Connected by Posts. NACA TN 2760, 1952.

4. Anderson, Roger A., Wilder, Thomas W., III, and Johnson, Aldie E., Jr.: Preliminary Results of Stability Calculations for the Bending of Box Beams With Longitudinally Stiffened Covers Connected by Posts. NACA RM L52K10a, 1952.

5. Anderson, Roger A., Johnson, Aldie E., Jr., and Wilder, Thomas W., III: Design Data for Multipost-Stiffened Wings in Bending. NACA TN 3118, 1954.

6. Badger, D. M.: Analysis and Design of Multipost-Stiffened Wings. Aero. Eng. Rev., vol. 12, no. 7, July 1953, pp. 45-57.

7. Rosen, B. Walter: Analysis of the Ultimate Strength and Optimum Proportions of Multiweb Wing Structures. NACA TN 3633, 1956.

8. Anderson, Roger A., and Anderson, Melvin S.: Correlation of Crippling Strength of Plate Structures With Material Properties. NACA TN 3600, 1956.

9. Hu, Pai C., Lundquist, Eugene E., and Batdorf, S. B.: Effect of Small Deviations From Flatness on Effective Width and Buckling of Plates in Compression. NACA TN 1124, 1946.

10. Schuette, Evan H., and McCulloch, James C.: Charts for the Minimum-Weight Design of Multiweb Wings in Bending. NACA TN 1323, 1947.

11. Pride, Richard A., and Anderson, Melvin S.: Experimental Investigation of the Pure-Bending Strength of 75S-T6 Aluminum-Alloy Multiweb Beams With Formed-Channel Webs. NACA TN 3082, 1954.

12. Semonian, Joseph W., and Anderson, Roger A.: An Analysis of the Stability and Ultimate Bending Strength of Multiweb Beams With Formed-Channel Webs. NACA TN 3232, 1954.

TABLE I

BEAM DIMENSIONS

Beam	h, in.	t_w, in.	t_s, in.	t_T, in.	b_s, in.	w, in.	c, in.	I, $in.^4$	A, sq in.	A_c, sq in. (1)
1	10.00	0.102	0.250	0.250	7.25	44.60	5.00	627	31.23	19.00
2	10.00	.102	.250	.250	7.25	44.60	5.00	641	30.77	18.07
3	10.01	.105	.256	.312	7.25	44.60	5.35	707	33.91	18.16
4	10.02	.106	.254	.314	7.26	45.15	5.38	746	36.75	20.35
5	10.00	.106	.255	.310	7.26	45.13	5.33	726	35.27	19.03
6	10.01	.106	.253	.314	7.25	45.12	5.38	721	34.96	18.48

[1]The designation A_c includes compression cover, webs, posts, and attachments (angle, tee, hat) on compression cover. It does not include tension cover and tension attachments.

REFERENCES

1. Johnson, Aldie E., Jr.: Bending Tests on Box Beams Having Solid- and Open-Construction Webs. NACA TN 3231, 1954.

2. Seide, Paul, and Barrett, Paul F.: The Stability of the Compression Cover of Box Beams Stiffened by Posts. NACA Rep. 1047, 1951. (Supersedes NACA TN 2153.)

3. Seide, Paul: Derivation of Stability Criterions for Box Beams With Longitudinally Stiffened Covers Connected by Posts. NACA TN 2760, 1952.

4. Anderson, Roger A., Wilder, Thomas W., III, and Johnson, Aldie E., Jr.: Preliminary Results of Stability Calculations for the Bending of Box Beams With Longitudinally Stiffened Covers Connected by Posts. NACA RM L52K10a, 1952.

5. Anderson, Roger A., Johnson, Aldie E., Jr., and Wilder, Thomas W., III: Design Data for Multipost-Stiffened Wings in Bending. NACA TN 3118, 1954.

6. Badger, D. M.: Analysis and Design of Multipost-Stiffened Wings. Aero. Eng. Rev., vol. 12, no. 7, July 1953, pp. 45-57.

7. Rosen, B. Walter: Analysis of the Ultimate Strength and Optimum Proportions of Multiweb Wing Structures. NACA TN 3633, 1956.

8. Anderson, Roger A., and Anderson, Melvin S.: Correlation of Crippling Strength of Plate Structures With Material Properties. NACA TN 3600, 1956.

9. Hu, Pai C., Lundquist, Eugene E., and Batdorf, S. B.: Effect of Small Deviations From Flatness on Effective Width and Buckling of Plates in Compression. NACA TN 1124, 1946.

10. Schuette, Evan H., and McCulloch, James C.: Charts for the Minimum-Weight Design of Multiweb Wings in Bending. NACA TN 1323, 1947.

11. Pride, Richard A., and Anderson, Melvin S.: Experimental Investigation of the Pure-Bending Strength of 75S-T6 Aluminum-Alloy Multiweb Beams With Formed-Channel Webs. NACA TN 3082, 1954.

12. Semonian, Joseph W., and Anderson, Roger A.: An Analysis of the Stability and Ultimate Bending Strength of Multiweb Beams With Formed-Channel Webs. NACA TN 3232, 1954.

TABLE I

BEAM DIMENSIONS

Beam	h, in.	t_w, in.	t_s, in.	t_T, in.	b_s, in.	w, in.	c, in.	I, $in.^4$	A, sq in.	A_C, sq in. (1)
1	10.00	0.102	0.250	0.250	7.25	44.60	5.00	627	31.23	19.00
2	10.00	.102	.250	.250	7.25	44.60	5.00	641	30.77	18.07
3	10.01	.105	.256	.312	7.25	44.60	5.35	707	33.91	18.16
4	10.02	.106	.254	.314	7.26	45.15	5.38	746	36.75	20.35
5	10.00	.106	.255	.310	7.26	45.13	5.33	726	35.27	19.03
6	10.01	.106	.253	.314	7.25	45.12	5.38	721	34.96	18.48

[1]The designation A_C includes compression cover, webs, posts, and attachments (angle, tee, hat) on compression cover. It does not include tension cover and tension attachments.

TABLE II

TEST RESULTS

Beam	M_f, in-kips	$M_{f,calc}$, in-kips	$\frac{M_{f,calc}}{M_f}$	$\frac{\sqrt{M_f}}{A_c}$
1	6,500	6,640	1.02	4.25
2	6,940	6,850	.99	4.62
3	7,520	7,090	.94	4.79
4	7,480	7,410	.99	4.25
5	7,740	7,360	.95	4.76
6	7,580	7,190	.95	4.70

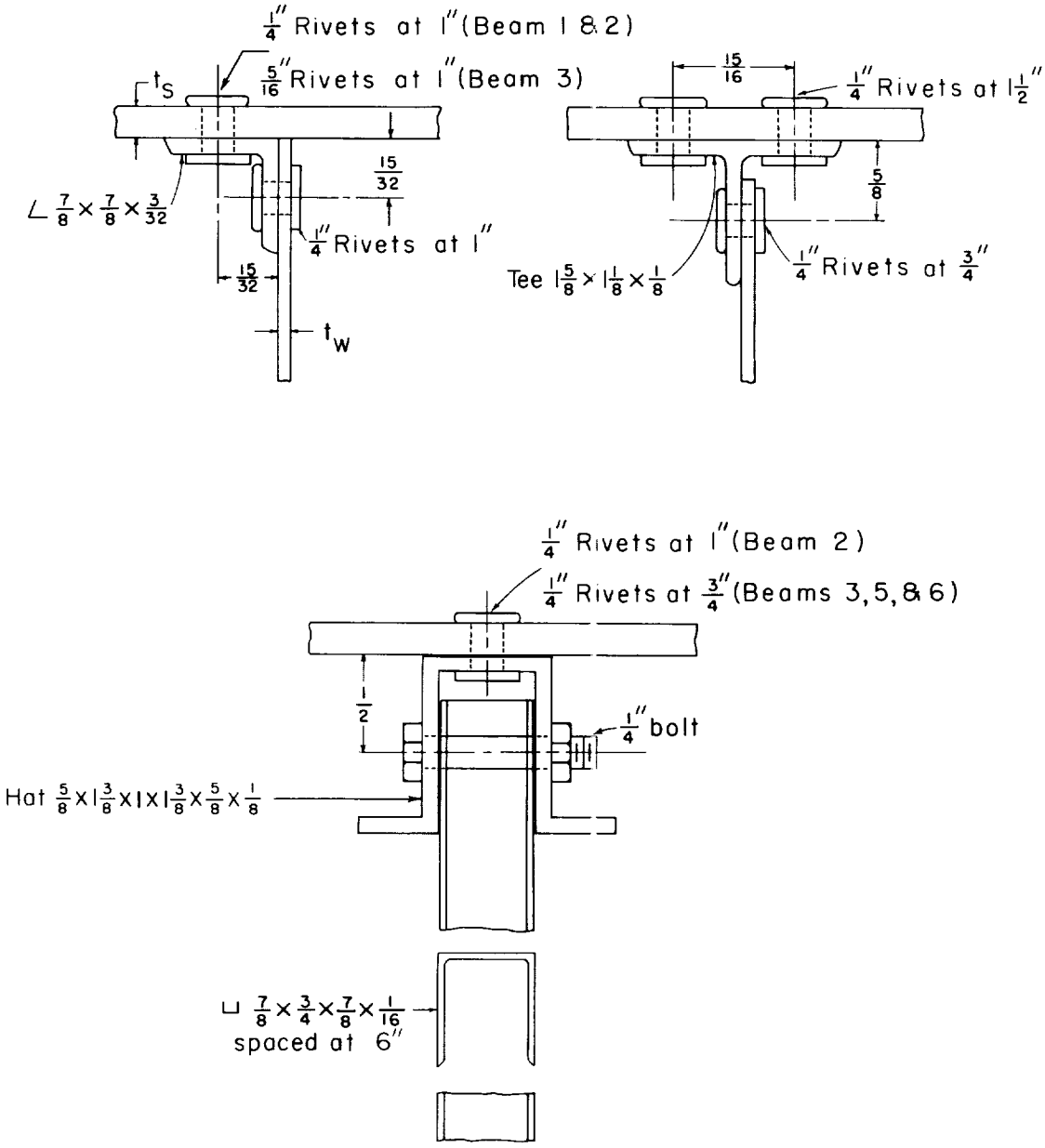

Figure 1.- Webs used in test beams.

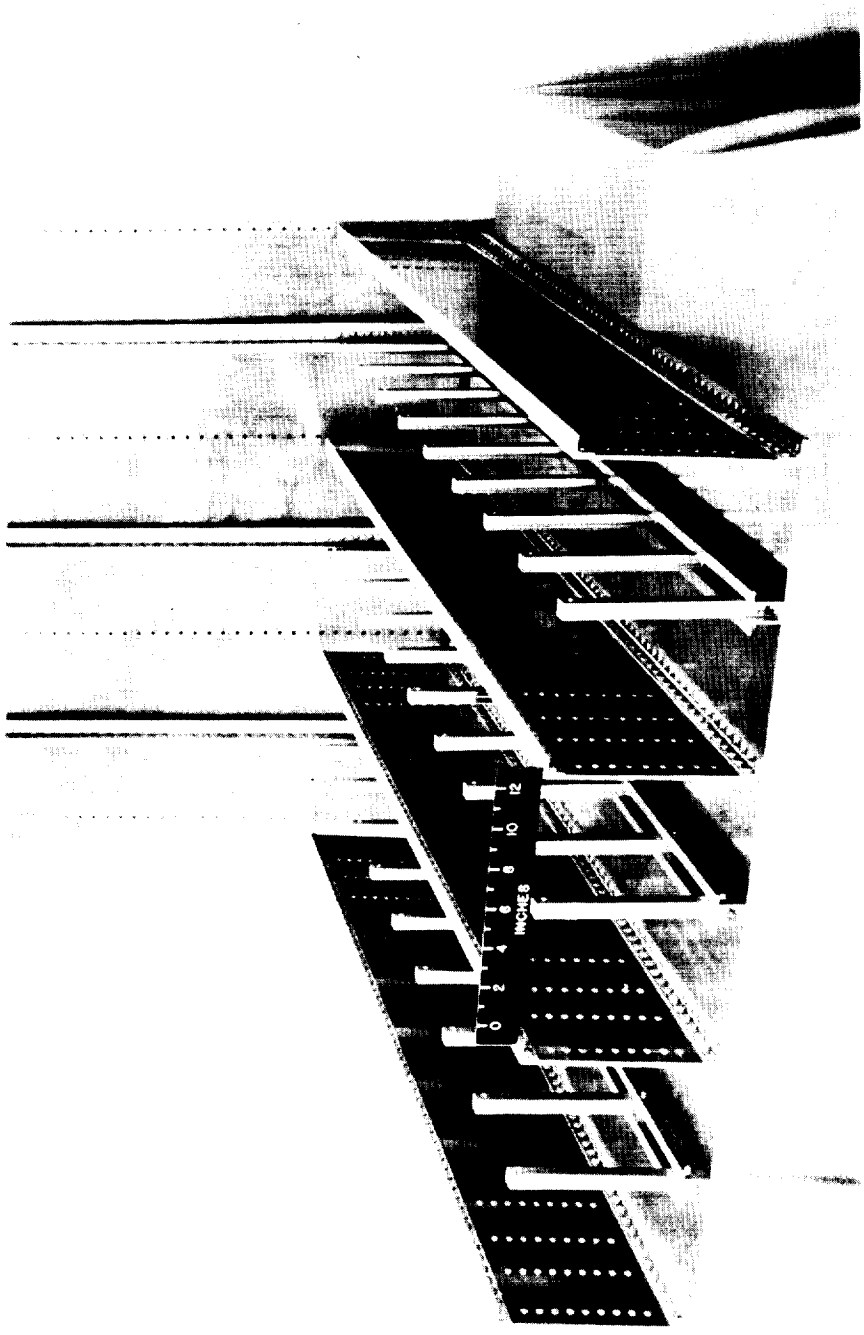

Figure 2.- Internal construction of beam 2. L-89485.1

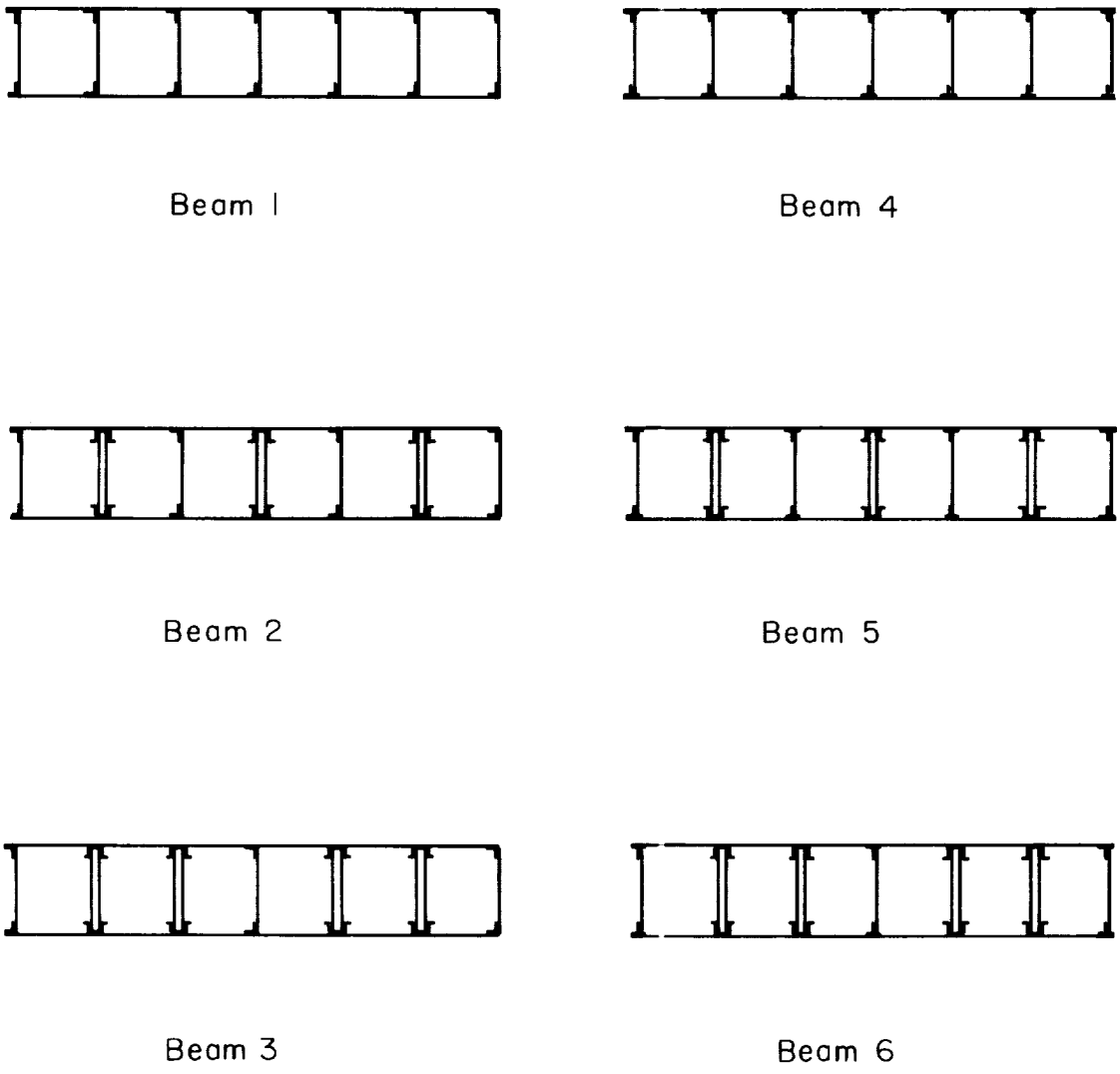

Figure 3.- Arrangement of webs in test beams.

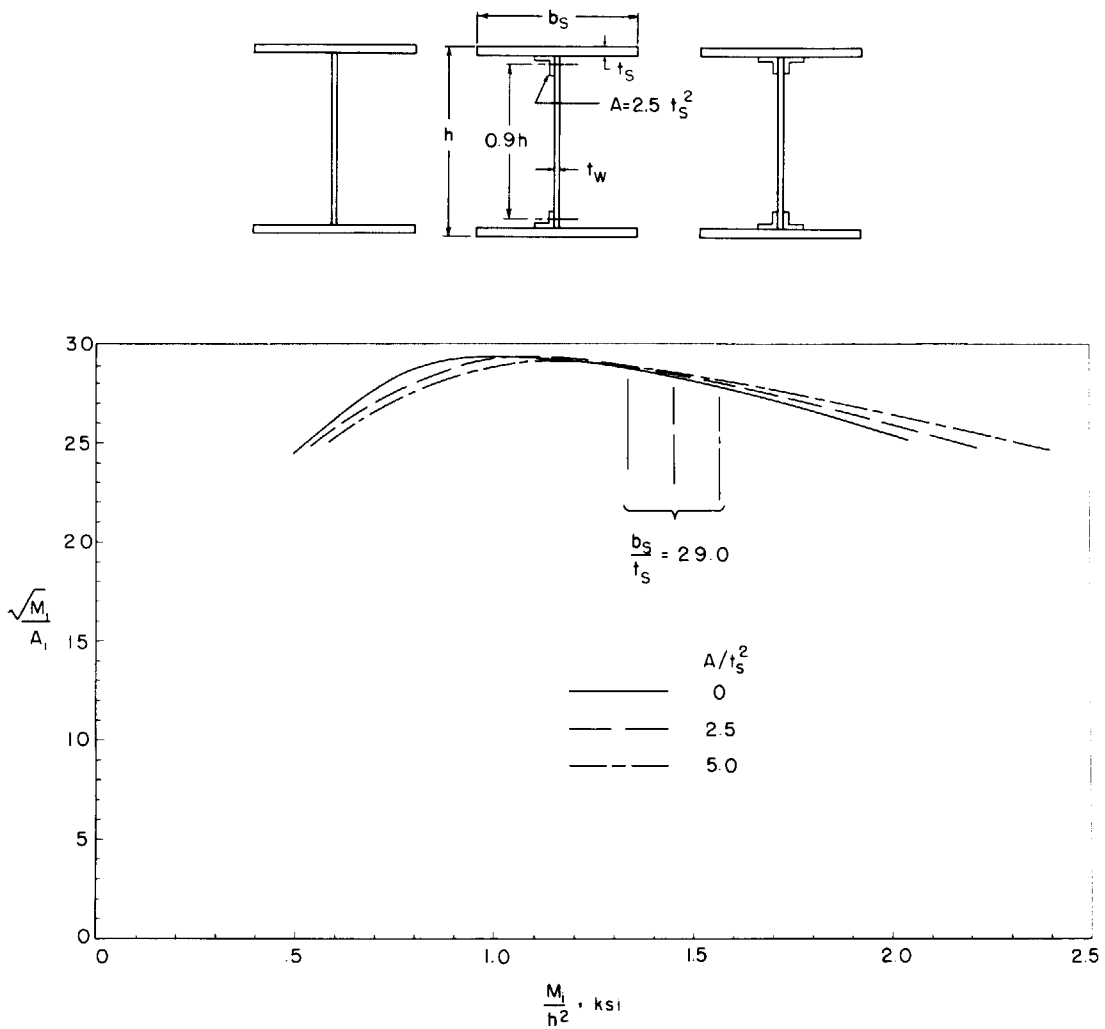

Figure 4.- Efficiency diagram for beams with a ratio of beam depth to compression-cover thickness of 40.

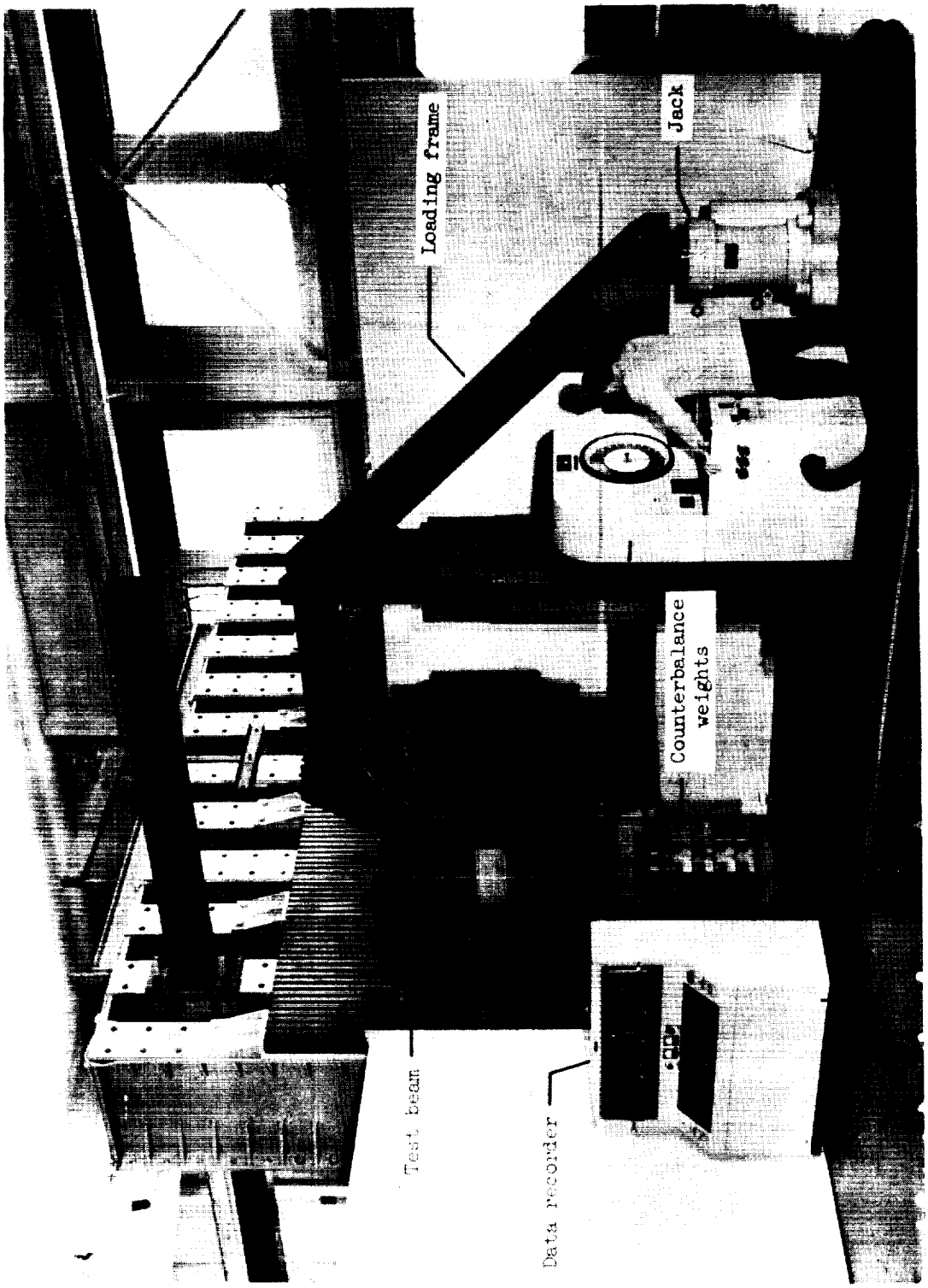

Figure 5.- Test setup for beams 1 and 2. L-93190.1

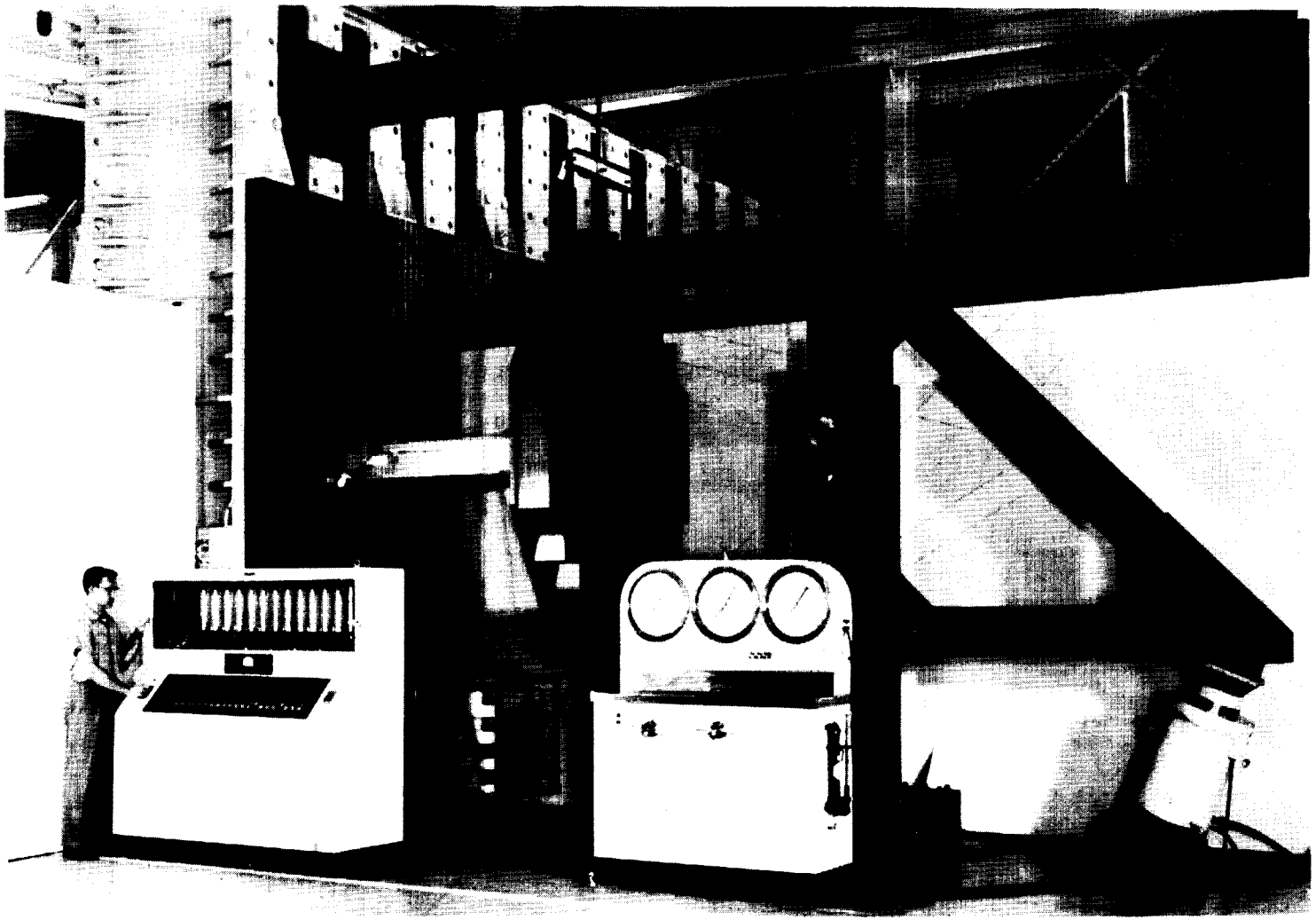

Figure 6.- Test setup for beams 3 to 6. L-57-2912.1

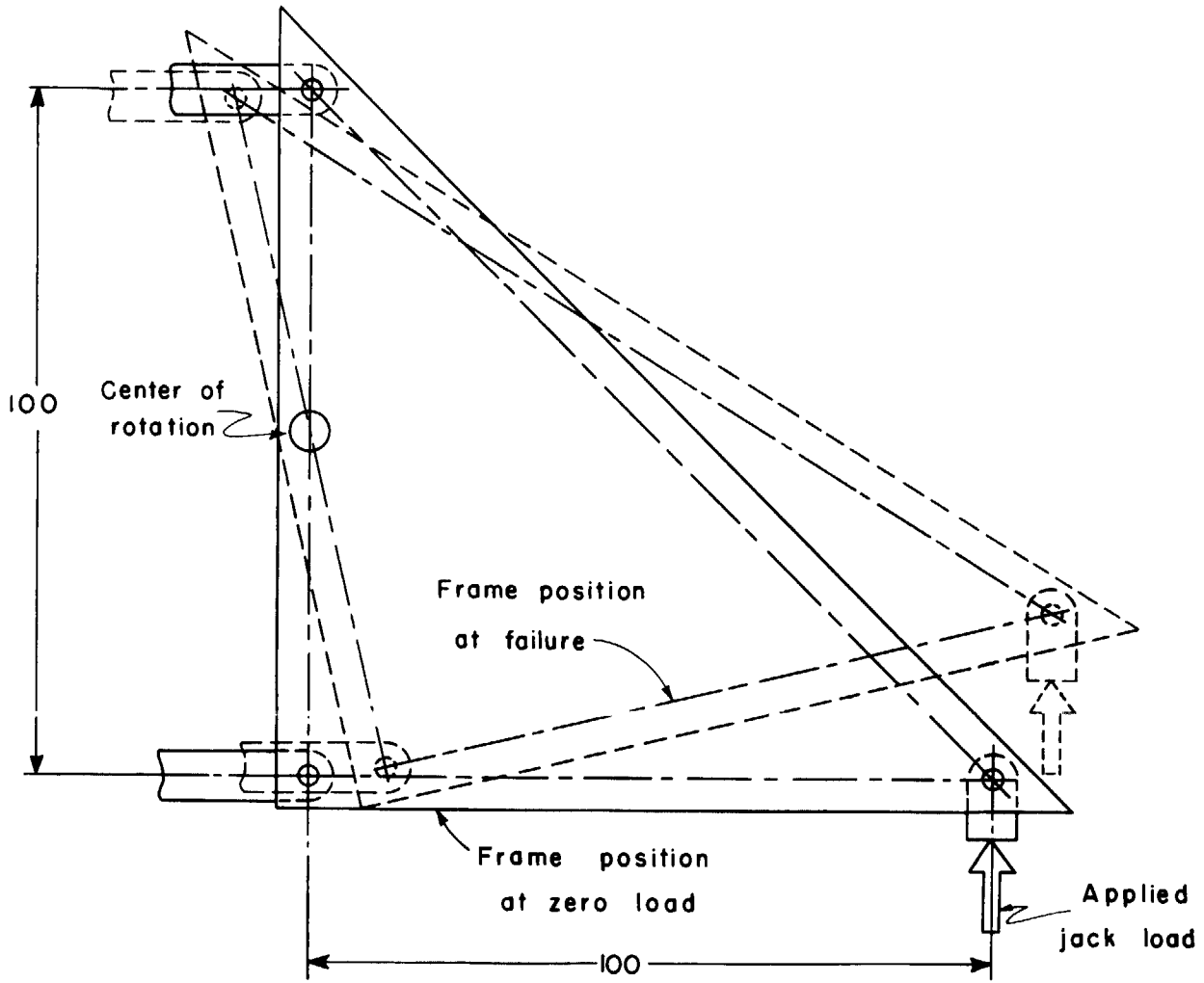

Figure 7.- Schematic diagram showing the relationship between loading-pedestal translation and loading-frame rotation.

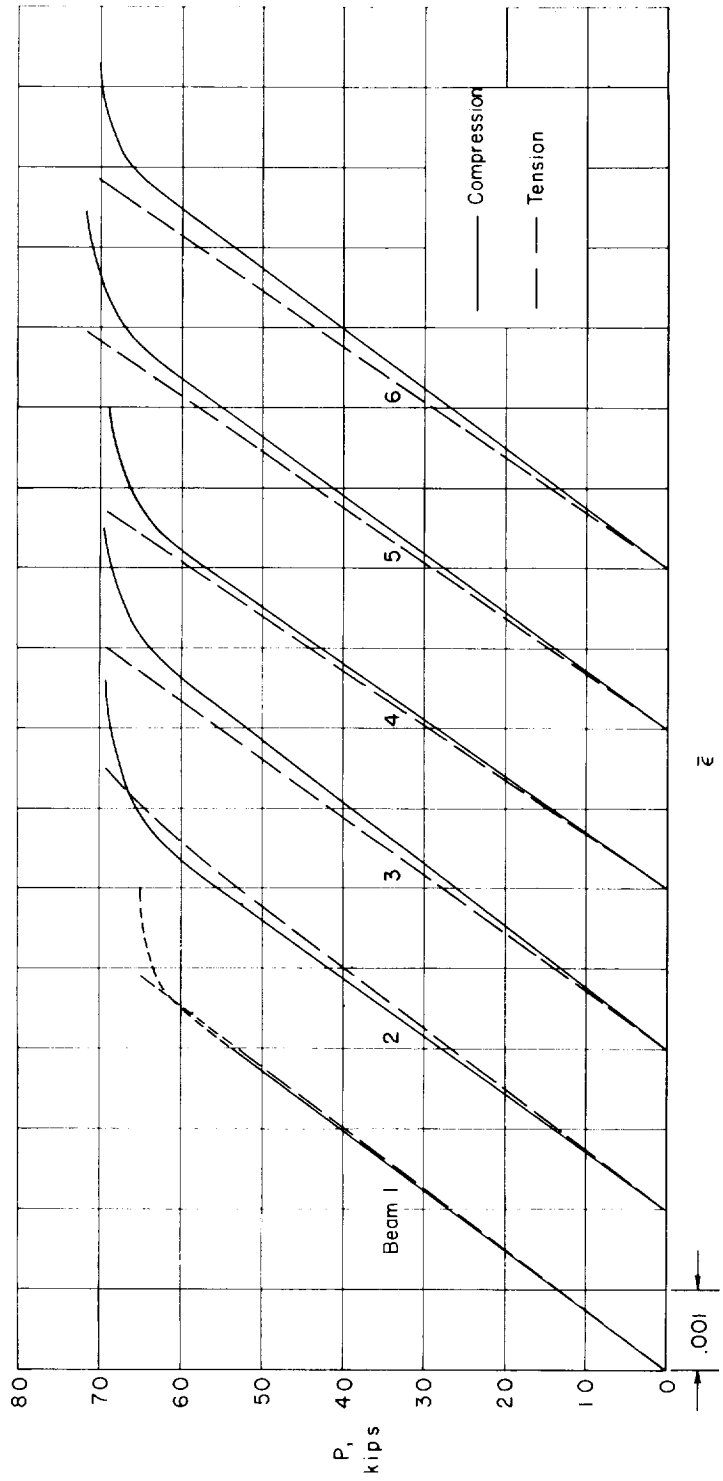

Figure 8.- Load-shortening diagrams of the tension and compression covers of test beams.

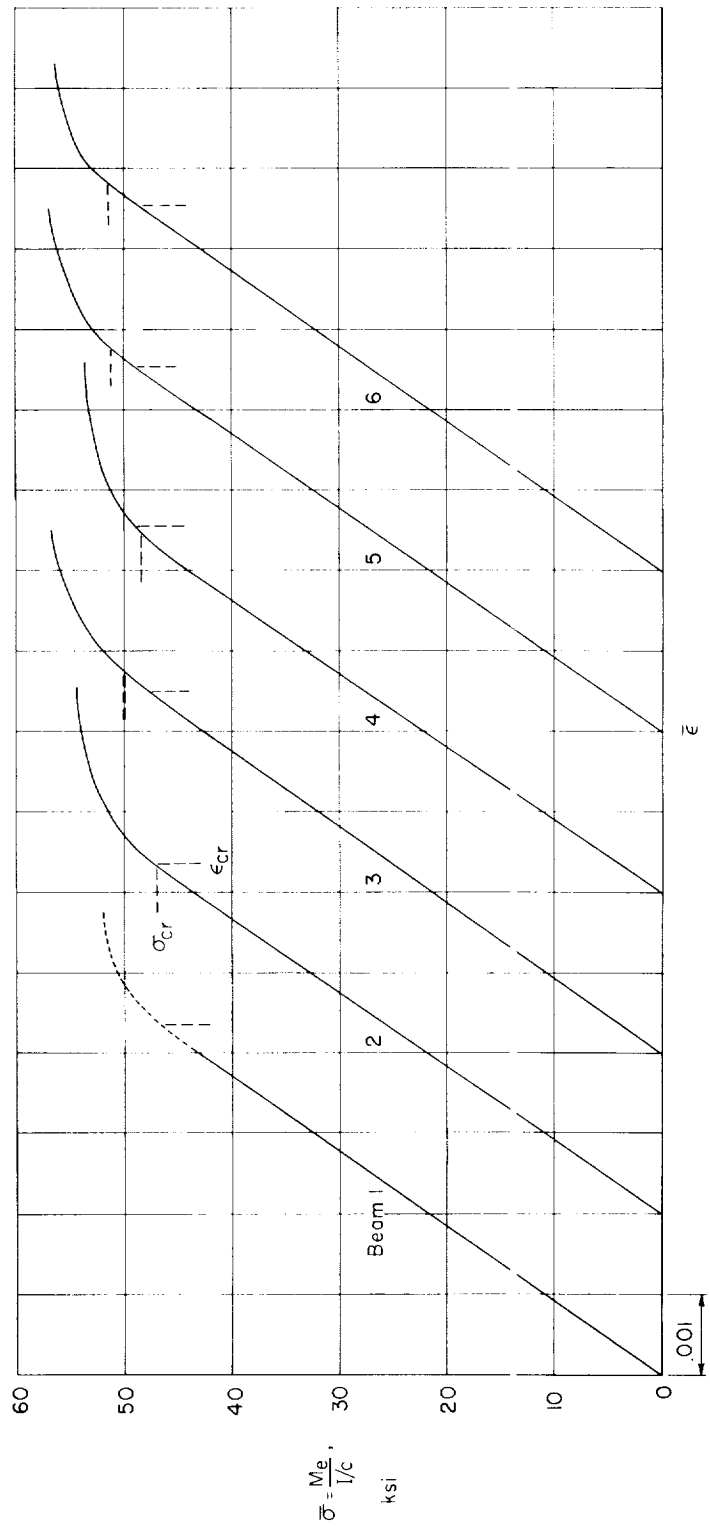

Figure 9.- Alternate form of load-shortening diagram for compression cover of test beams.

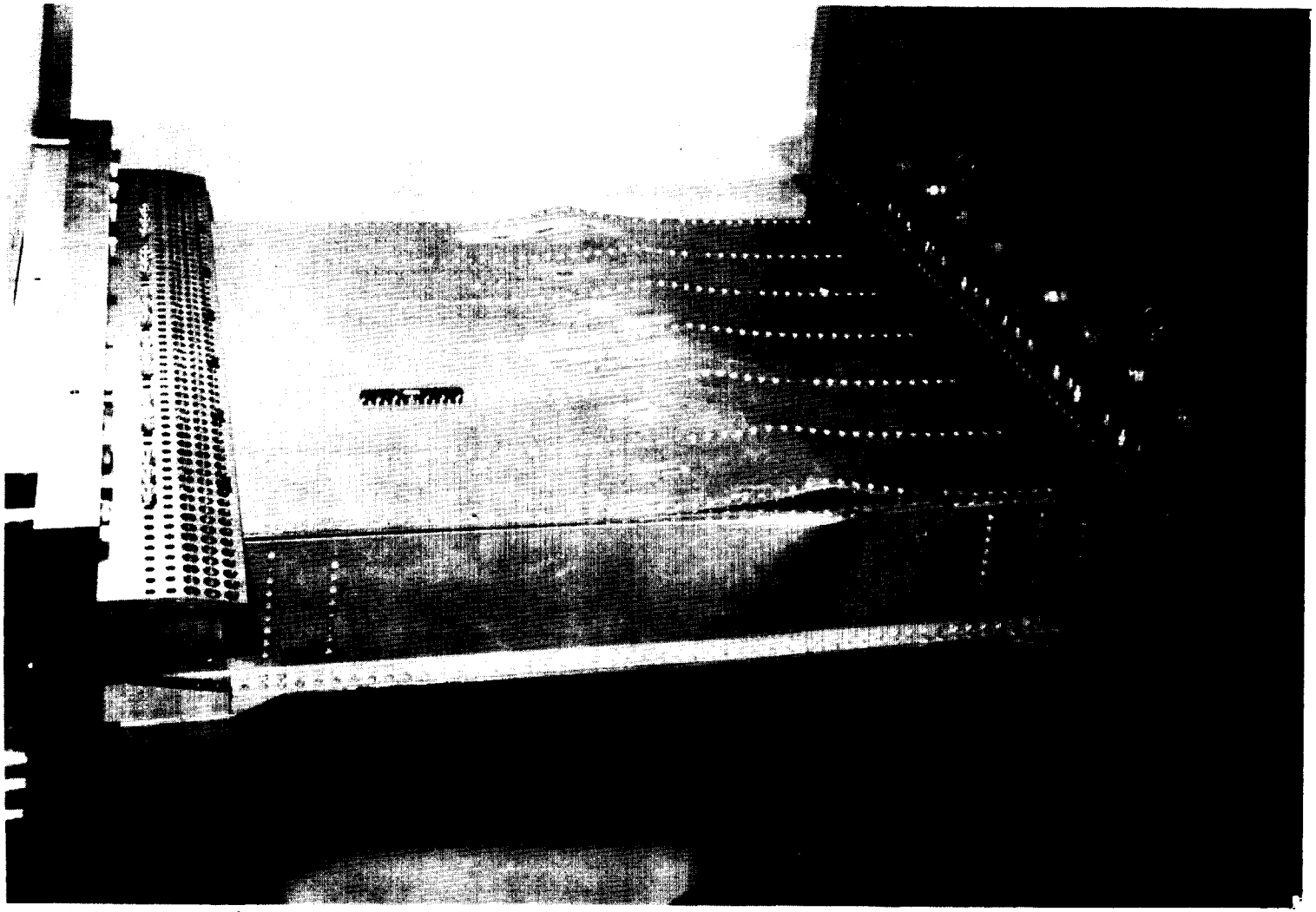

Figure 10.- Failure of beam 1. L-93051

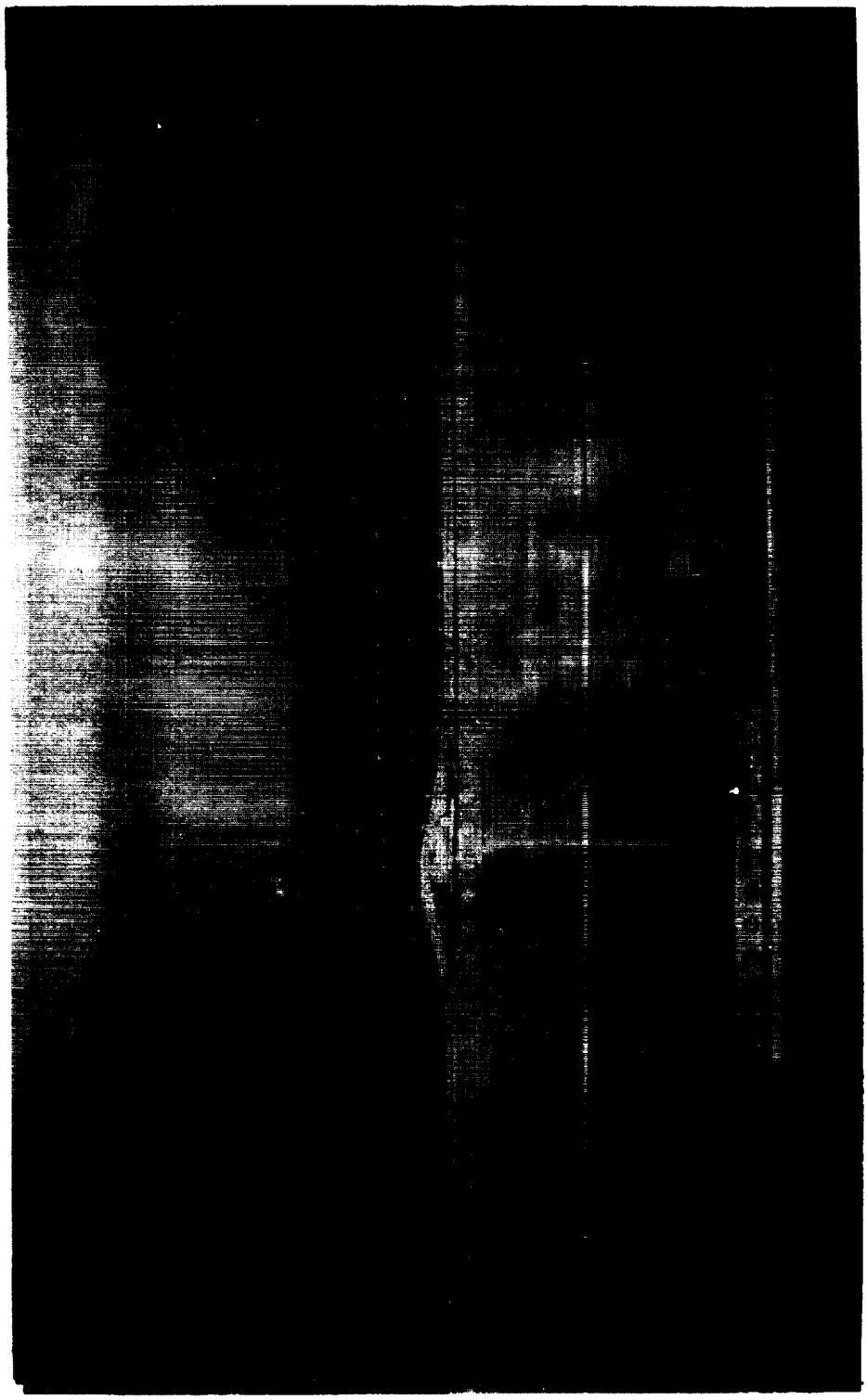

Figure 11.- Failure of beam 2. L-93288

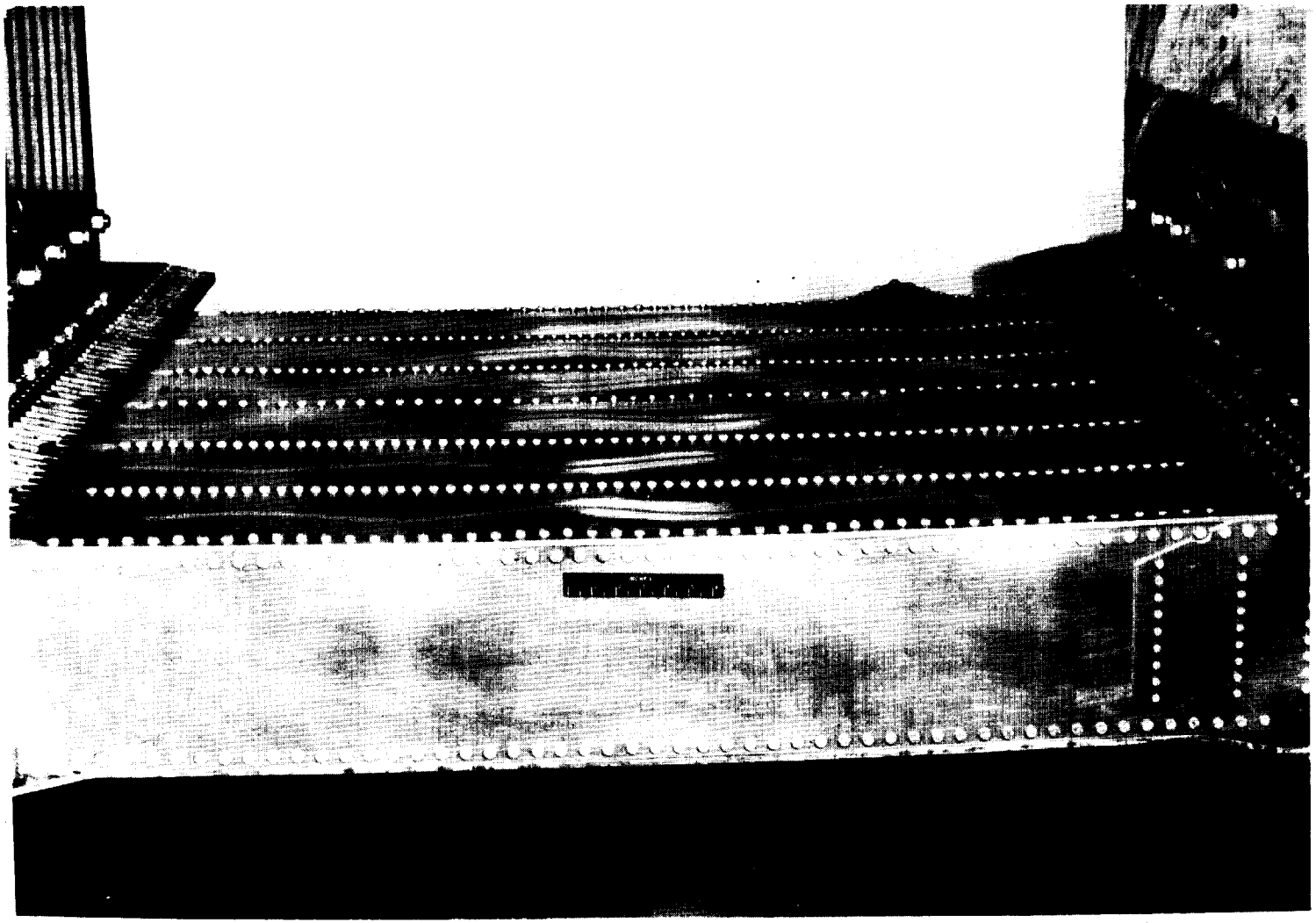

Figure 12.- Failure of beam 3. L-57-2878

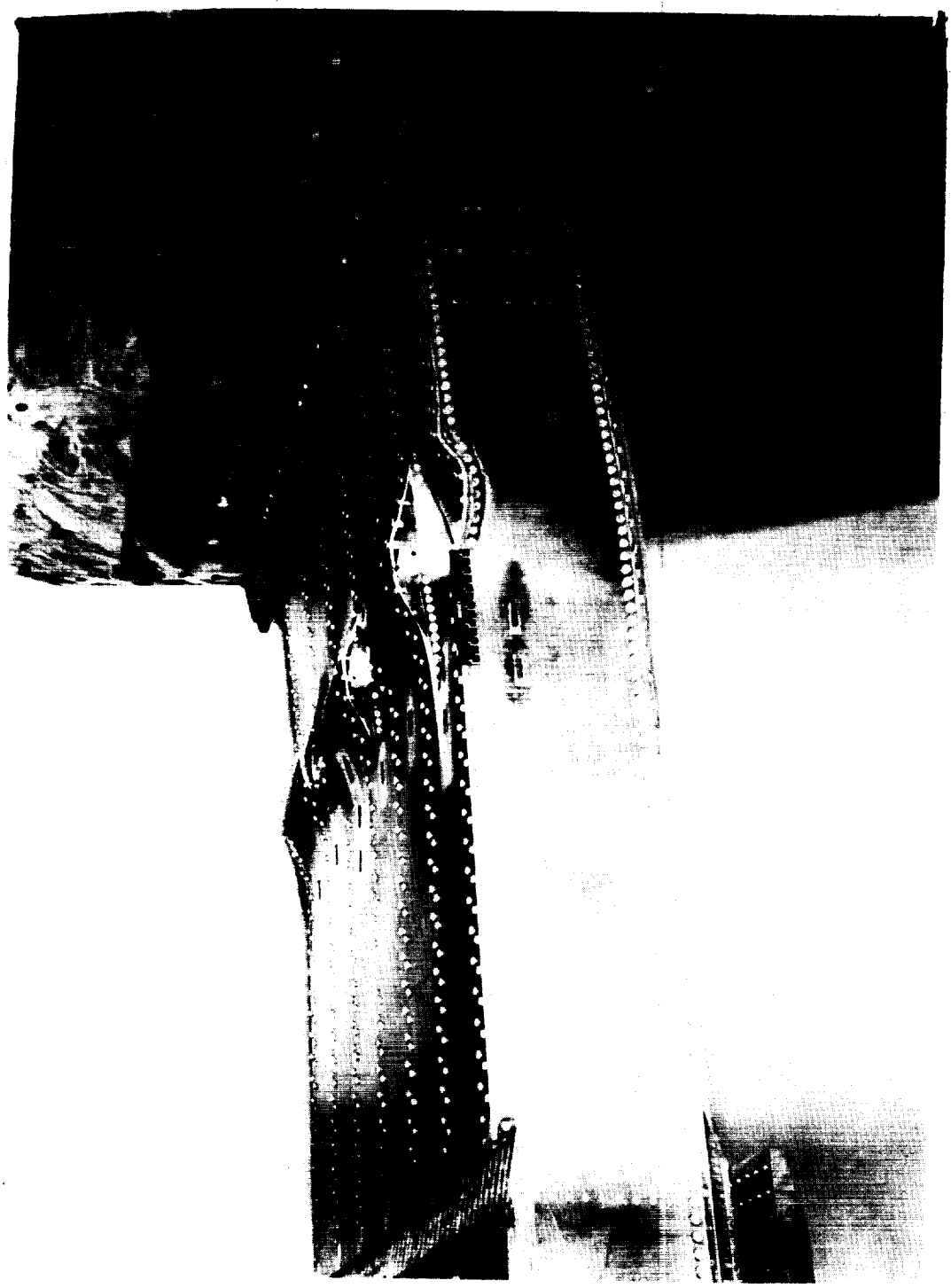

Figure 13.- Failure of beam 4. L-57-3008

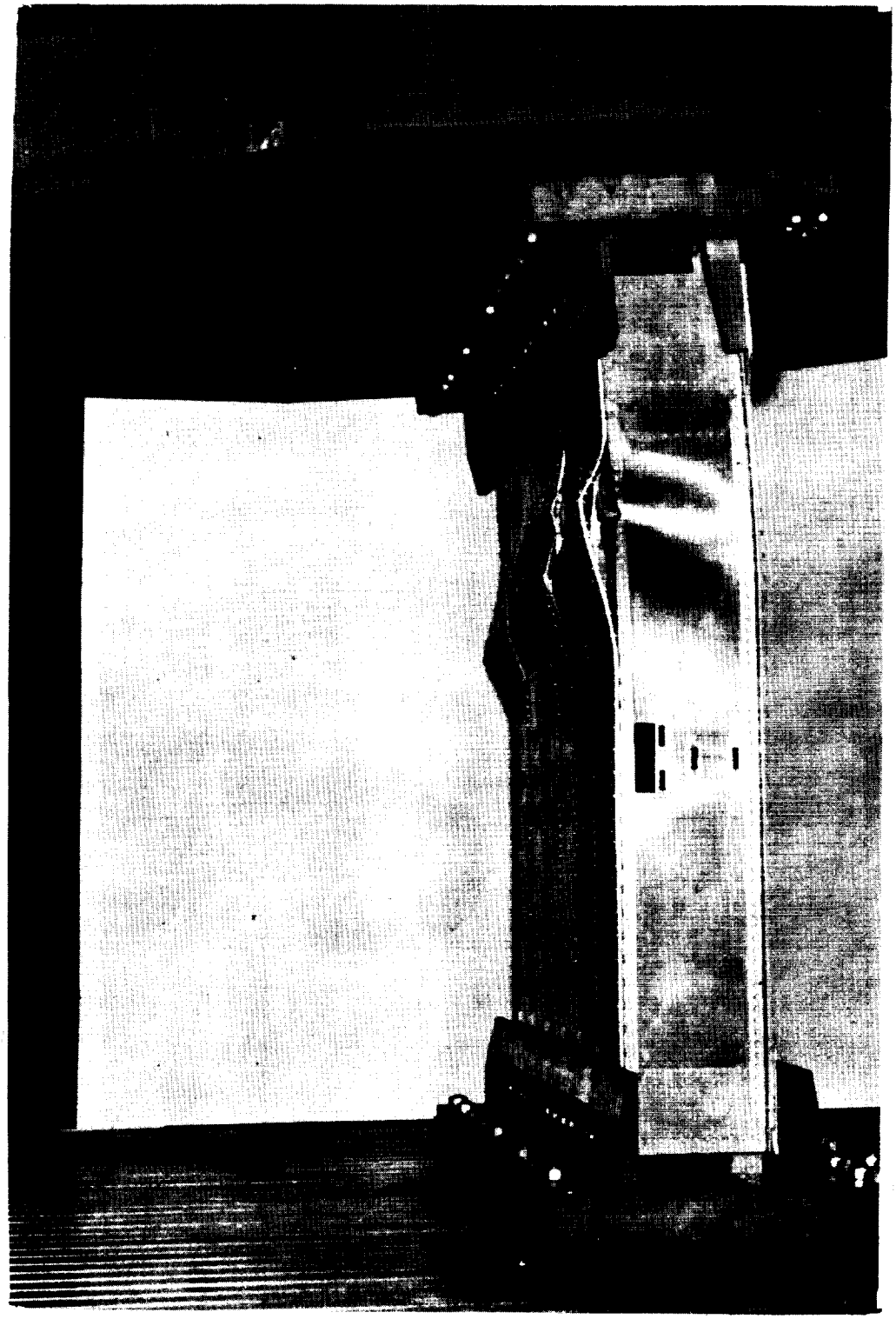

Figure 14.- Failure of beam 5. L-57-5281.1

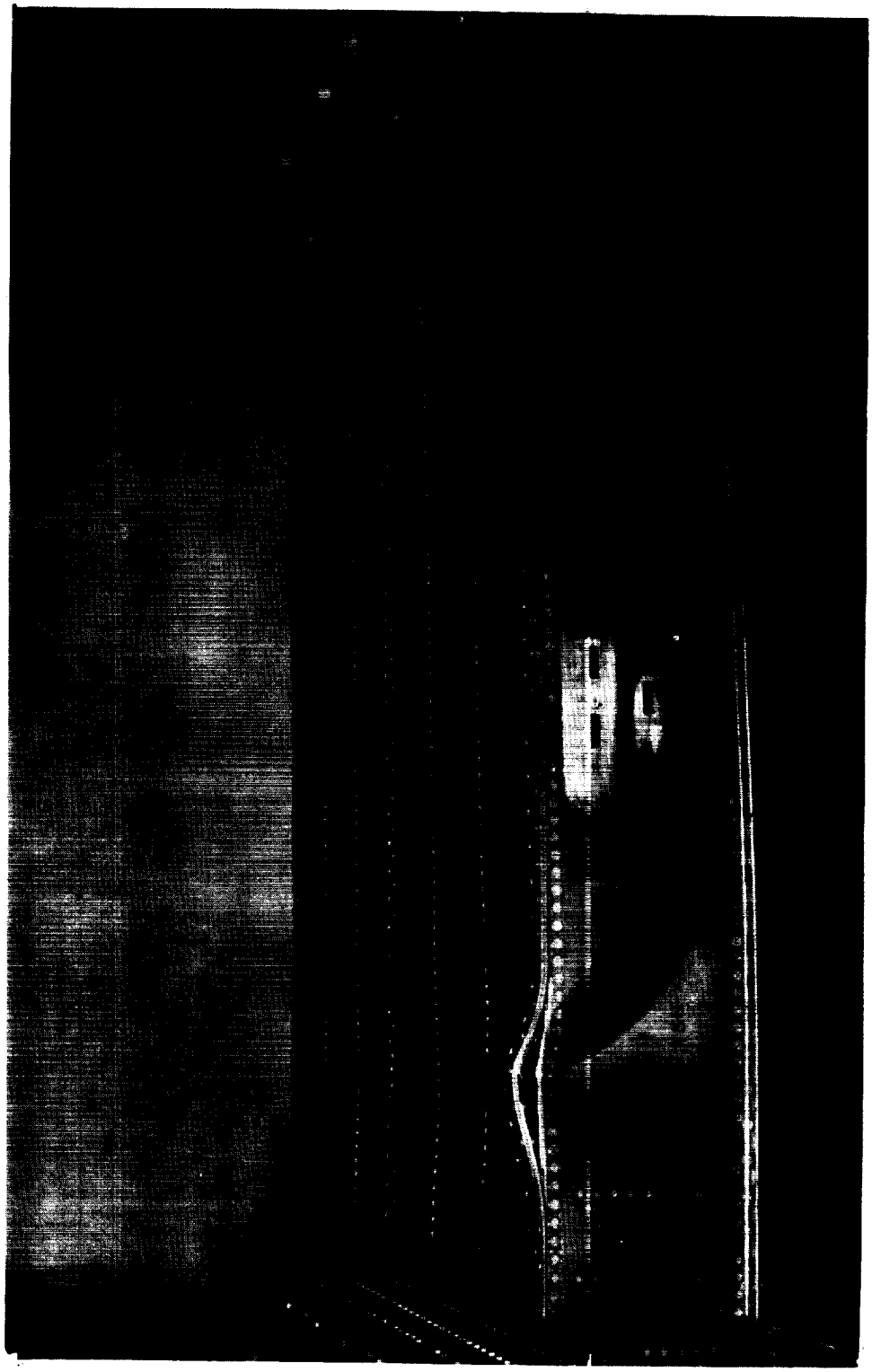

Figure 15.- Failure of beam 6. L-57-3127

NASA - Langley Field, Va. L-385